arXiv:astro-ph/0002399v1 21 Feb 2000

The Detection of the Diffuse Interstellar Bands in Dusty Starburst Galaxies

Timothy M. Heckman[1]
Department of Physics and Astronomy, Johns Hopkins University, Homewood Campus, 3400 North Charles Street, Baltimore, MD 21218

Matthew D. Lehnert[1]
Max-Plank-Institut für extraterrestrische Physik, Postfach 1603, D-85740 Garching, Germany

1. Visiting astronomers, Kitt Peak National Observatory and Cerro Tololo Interamerican Observatory, NOAO, operated by AURA, Inc. under cooperative agreement with the National Science Foundation.

ABSTRACT

We report the detection of the Diffuse Interstellar Bands ("$DIBs$") in the optical spectra of seven far-infrared-selected starburst galaxies. The λ6283.9 Å and λ 5780.5 Å features are detected with equivalent widths of $\sim$ 0.4 to 1 Å and 0.1 to 0.6 Å respectively. In the two starbursts with the highest quality spectra (M82 and NGC2146), four other weaker $DIBs$ at λ 5797.0 Å, 6010.1 Å, 6203.1 Å, and 6613.6 Å are detected with equivalent widths of $\sim$ 0.1 Å. The region over which the $DIBs$ can be detected ranges from $\sim$ 1 kpc in the less powerful starbursts, to several kpc in the more powerful ones. The gas producing the $DIBs$ is more kinematically quiescent on-average than the gas producing the strongly-blueshifted $NaI\lambda\lambda$5890,5896 absorption in the same starbursts. We show that the $DIBs$ in these intense starbursts are remarkably similar to those in our Galaxy: the relative strengths of the features detected are similar, and the equivalent widths follow the same dependence as Galactic $DIBs$ on $E(B-V)$ and NaI column density. While the ISM in starbursts is heated by a photon and cosmic ray bath that is $\sim 10^3$ times more intense than in the diffuse ISM of the Milky Way, the gas densities and pressures are also correspondingly larger in starbursts. This "homology" may help explain the strikingly similar DIB properties.

Subject headings: Galaxies: Starburst – Galaxies: Nuclei – Galaxies: ISM – ISM: Molecules – ISM: Dust,Extinction – Line: Identification

1. Introduction

The Diffuse Interstellar Bands ("$DIBs$") have been studied for over 60 years, since Merrill (1934) first established their origin in the interstellar medium. Despite decades of intensive investigation, the identity of the carrier or carriers of the $DIBs$ has not been established (see the comprehensive review by Herbig 1995). The most likely candidates are large carbon-rich molecules (e.g. Sonnentrucker et al 1997), perhaps Polycyclic Aromatic Hydrocarbons (PAH's - Salama et al 1999). The strongest and best-studied $DIBs$ in the optical spectrum are known empirically to trace the HI phase of the ISM, with strengths that correlate well with the line-of-sight color excess $E(B-V)$, the HI column density, and the NaI column density as probed with the $NaI\lambda\lambda$5890,5896 ("NaD") doublet (see Herbig 1993).

To date, $DIBs$ have been observed almost exclusively in our own Galaxy, and to a limited extent in the Magellanic Clouds (Morgan 1987). Supernova 1986G in NGC 5128 (Cen A) allowed the detection of $DIBs$ produced within the famous dusty gas disk in this elliptical galaxy (di Serego Alighieri & Ponz 1987). Most recently, Gallagher & Smith (1999) have reported the possible discovery of the DIB at λ6283.9 Å in the spectra of two "super starclusters" near the nucleus of the prototypical starburst galaxy M 82. This is intriguing, since it suggests that the DIB carriers are present at a normal level even in the ISM of an intense starburst, in which the ambient radiation intensity and gas pressure are orders-of-magnitude higher than in the diffuse gas in the Milky Way disk (e.g. Colbert et al 1999).

We have recently analyzed the properties of the interstellar NaD absorption- line in the spectra of 18 high-luminosity, infrared-selected (dusty) starbursts (Heckman et al. 2000 - hereafter HLSA). In the course of this analysis, we examined the 7 starbursts with the highest quality spectra for the presence of $DIBs$ (section 2). As we report in section 3 below, we have detected one or both of the λ6283.9 Å and λ5780.5 Å DIB features (normally the two strongest $DIBs$ in the optical spectral region) in all seven cases. We have also been able to map the spatial distribution of the $DIBs$. These data allow us to directly compare the properties of the $DIBs$ in the ISM of these extreme starbursts to sight-lines in the Galaxy having similar gas column density and reddening (section 4).

2. Observations & Data Analysis

Details concerning the following are given in HLSA, so we only summarize the most salient points here.

The starburst sample presented here is a subset of the 32 galaxies observed by HLSA. The HLSA sample itself was selected from two far-infrared-bright samples: the Armus, Heckman, & Miley (1989) sample of galaxies with very warm far-IR colors and the Lehnert & Heckman (1995) sample of far-IR-bright disk galaxies seen at high inclination. The combined sample is representative of the far-IR-galaxy phenomenon, but is not complete.

HLSA found that the NaD line was of predominantly interstellar origin in 18 of the 32 galaxies, while cool stars contributed significantly to the line in the other 14 cases. The plethora of weak absorption features in the spectra of cool stars greatly complicate the detection of the $DIBs$, while the strength of $DIBs$ in our Galaxy correlate strongly with the ISM NaI column density. Thus, the galaxies in the present paper were drawn exclusively from the 18 "interstellar-dominated" objects in HLSA. We then selected the objects in HLSA having the highest signal-to-noise spectra obtained with a resolution better than ~ 100 km s^{-1} (see below). This results in a sample of 7 galaxies, as listed in Table 1.

The observations were undertaken in 1993 and 1994 using two different facilities: the 4-meter Blanco Telescope with the Cassegrain Spectrograph at $CTIO$ and the 4-meter Mayall Telescope with the RC Spectrograph at $KPNO$. The spectral resolution ranged from 1.1 Å FWHM in the $KPNO$ data to 1.8 Å FWHM in the $CTIO$ data. Details regarding spectrograph configurations are listed in Table 2 of HLSA.

The spectra were all processed using the standard $LONGSLIT$ package in $IRAF$ (bias-subtracted, flat-fielded using spectra of a quartz-lamp, geometrically-rectified and wavelength-calibrated using a $HeNeAr$ arc lamp, and then sky-subtracted). See HLSA for details. No explicit correction was made for the presence of weak telluric absorption-features, but these are not a problem for our analysis. The strongest feature of relevance is the O_2 band from ~ 6276 to 6284 Å (e.g. Figure 2a in Benvenuti & Porceddu 1989). Fortunately, the redshifts of our galaxies are sufficient to move the λ6283.9 Å DIB out from under this feature.

The spectra were analyzed using the interactive $SPLOT$ spectral fitting package in $IRAF$. In all cases, a one-dimensional "nuclear" spectrum was extracted, covering a region with a size set by the slit width and summed over 5 pixels in the spatial direction (the resulting aperture is typically 2 by 4 arcsec). The corresponding linear size of the projected aperture is generally a few hundred parsecs to a few kpc in these galaxies (median diameter 600 pc). This is a reasonable match to the typical sizes of powerful starbursts like these (e.g. Meurer et al 1997; Lehnert & Heckman 1996). Prior to further analysis, each 1-D spectrum was normalized to unit intensity by fitting it with, and then dividing it by, a low-order polynomial. Similar one-dimensional spectra for off- nuclear regions were extracted over the spatial region with adequate signal- to-noise in the continuum for each galaxy.

It is essential to remove the myriad absorption features due to cool stars from the spectra before searching for the relatively weak DIB features. We have therefore used the average spectrum of several Galactic K giant stars as a template. After redshifting the normalized stellar template to the galaxy rest-frame, we have iteratively scaled and subtracted the template from the normalized galaxy spectrum until the residuals in the difference spectrum were minimized in the spectral regions that exclude potentially detectable interstellar features. The scale factors found for the stellar template imply that cool stars typically contribute 20 to 30% of the continuum light at $\sim$ 6000Å. This is consistent with both the less rigorous estimates reported in HLSA for these galaxies, and with theoretical expectations for red supergiants in a mature metal-rich starburst (Bruzual & Charlot 1993; Leitherer et al 1999). To compensate for the effects of the continuum subtraction, we added back an equivalent amount of featureless continuum. Thus, the depths and equivalent widths of the $DIBs$ in the original data are preserved by our analysis. As an example, we show the spectrum of the nucleus of M82 before and after the subtraction of a suitably-scaled K-star spectrum in Figure 1. These final processed spectra are shown in Figures 2 and 3.

We have estimated the uncertainties in our measurements in two ways. First, we compared the measurements for the four galaxies in the sample for which we have more than one independent spectrum (taken at a different position angle). Second, we have calculated the rms noise in the cool-star-subtracted spectra and used this to calculate the implied uncertainties (assuming standard error propogation for Poissonian noise). We report these uncertainties in Tables 1 through 3.

3. Results

3.1. The Identified Features

The two most conspicuous $DIBs$ along typical sight-lines in the ISM of our Galaxy are the strong, relatively narrow features at λ6283.9 Å and λ5780.5 Å (Herbig 1995). In all but one case, both features are within the wavelength coverage of our spectra. The next strongest $DIBs$ in the Milky Way in the relevant spectral region are at 5797.0 Å, 6010.1 Å, 6203.1 Å, and 6613.6 Å. We have searched for all these features in our spectra.

We turn our attention first to the λ6283.9 Å feature, which is the strongest feature in the Milky Way, and is not seriously confused by stellar photospheric lines in the starburst spectra. As can be seen in Figure 2, the λ6283.9 DIB is detected in 6 of the 7 starburst nuclei (Table 1). The only exception is NGC 6240, where the feature would lie within the

blue shoulder of the very strong and broad [OI]λ6300 nebular emission-line, making it very difficult to detect. In the other six cases, the equivalent width of this DIB ranges from $\sim$ 0.4 to 0.9 Å with a normalized residual intensity at line-center of 0.83 to 0.94. These values correspond to some of the strongest features seen along sight-lines in the ISM of the Milky Way (e.g. Chlewicki et al 1986; Benvenuti & Porceddu 1989).

Weaker absorption due to the λ5780.5 DIB is definitely present in three of the seven members of our sample (NGC2146, M82, and NGC6240), and possibly present in three more (NGC1614, NGC1808, and NGC3256). No measurement can be made in IRAS10565+2448, since the feature lies just outside our spectral passband. In the five cases in which both features are detected, the λ5780.5 DIB is typically about 25% as strong as the λ6283.9 feature, compared to a mean value of about 45% along comparably-reddened lines-of-sight in the Milky Way (Chlewicki et al 1986; Benvenuti & Porceddu 1989). We emphasize that the measurement of the λ5780.5 DIB is difficult in our spectra owing to its proximity to the comparably strong stellar photospheric CrI+CuIλ5782 feature (with which it is badly blended). We estimate that this introduces an uncertainty of $\pm$ 50 mÅ in the quoted equivalent widths (which is generally larger than the formal measurement uncertainties estimated above).

The two starburst nuclei with the strongest λ6283.9 Å DIB feature are NGC 2146 and M82. These two spectra also have the highest signal-to-noise and (along with IRAS10565+2448) have the best spectral resolution and broadest wavelength coverage in our sample. In these two spectra, several other weaker DIB features can be identified, namely those at 5797.0 Å, 6010.1 Å, 6203.1 Å, and 6613.6 Å (Figure 3). The equivalent widths of these features are $\sim$100 mÅ or typically 10 to 15% as large as those of the λ6283.9 Å feature. These relative strengths agree reasonably well with Galactic $DIBs$ (Chlewicki et al 1986; Benvenuti & Porceddu 1989; Herbig 1995). We summarize this information in Table 2, and note that similarly-weak features could be present in the noisier spectra of the other five members of our sample.

3.2. Kinematics

We have measured the width and centroid of the λ6283.9 Å DIB feature in all cases but NGC 6240 (where we have instead used the λ5780.5 Å DIB). The measured line widths (Table 3) range from $\sim$ 5 to 9 Å. The intrinsic width of the λ6283.9 (λ5780.5) DIB in the Milky Way is $\sim$ 4 (2) Å (Herbig 1995). Taking our instrumental resolution into account, the implied Doppler broadening of the $DIBs$ due to macroscopic motions in the starburst ISM ranges from FWHM 160 to 430 km s^{-1}. In four of the seven cases, these Doppler widths are

smaller than the widths of the NaD doublet (by 25 to 60%). In NGC1808, NGC2146 and M82, the DIB NaD lines have the roughly the same Doppler widths. Interestingly, HLSA find that these are the three cases in the present sample in which the nuclear NaD lines do not show significant blueshifts with respect to the galaxy systemic velocity (v_{sys}).

The centroids of the $DIBs$ are within $\sim$ 100 km s^{-1} of v_{sys}. However, in all four cases with strongly blueshifted NaD lines (NGC1614, NGC3256, IRAS10565+2448, and NGC6240), the $DIBs$ are mildly blueshifted (by $\sim$ 50 to 110 km s^{-1}) with velocities that are intermediate between v_{NaD} and v_{sys}. The velocities of the DIB and NaD absorbers roughly agree with one another (and lie close to v_{sys}) in the other three cases. This kinematic information is summarized in Table 3.

Taken together, these results suggest that the $DIBs$ trace gas that is more quiescent on-average than that probed by the NaD line. That is, the NaD absorption in the four "outflow" nuclei is probably produced by a combination of quiescent material ($v \sim v_{sys}$ with smaller Doppler width) and disturbed, outflowing material. The bulk of the DIB absorption would be associated with the former, and this component would dominate both the NaD and DIB absorption in the three other cases in our sample.

3.3. Spatial Extent

We have used our long-slit data to map the extra-nuclear spatial extent of the $DIBs$ in these galaxies. As listed in Table 1, these sizes range from $\sim$ 1 to 6 kpc. The absorbing region is larger (3 to 6 kpc) in the more powerful starbursts (NGC1614, NGC3256, IRAS10565+2448, and NGC6240, with $logL_{bol}$ = 11.3 to 12.0 $L_{\odot}$), and smaller (0.9 to 1.8 kpc) in the less powerful cases (NGC1808, NGC2146, and M82, with $logL_{bol}$ = 10.5 to 10.7 $L_{\odot}$). In the nearby (less powerful) starbursts, these sizes reflect the extent of the absorbing material. In the more distant (more powerful) starbursts, these sizes are lower limits set by the region with adequate signal-to-noise in the stellar continuum.

4. Discussion

4.1. Comparison to Galactic DIBs

The strengths of the prominent Galactic $DIBs$ correlate well with the column densities of both HI and NaI and with the reddening along the line-of-sight (e.g. Chlewicki et al 1986; Herbig 1993). This implies that the DIB carrier is most plausibly associated with

the cool atomic phase of the ISM. We can use the data discussed in HLSA to estimate the values for N_{NaI} and $E(B-V)$ in our sample of seven starbursts, to see if the $DIBs$ in our starburst sample obey the same empirical relations defined by the ISM of the Milky Way.

We follow HLSA and derive estimates for N_{NaI} using the average of the values obtained from the classical "doublet ratio" method (Spitzer 1968) and the variant described by Hammann et al (1997). We estimate the line-of-sight reddening to the stellar continuum using the observed colors compared to theoretical models for a starburst stellar population (Leitherer et al 1999; see HLSA for details). We list the results in Table 1.

Our best-measured DIB by-far is the strong λ6283.9 feature. The data compiled by Chlewicki et al (1986) and Benvenuti & Porceddu (1989) show that the mean ratio of the equivalent width of this feature and the color excess is $< W_{6284}/E(B-V) > = 1.2$ Å for heavily-reddened Galactic sight-lines. For our small starburst sample we find a similar result: $< W_{6284}/E(B-V) > = 0.8$ Å. This is shown in Figure 4 where we have plotted W_{6284} *vs.* $E(B-V)$ for a large sample of Galactic sight-lines using the extensive data compled by Herbig (1993). To compare our starburst data directly to this Galactic data we have converted the values given by Herbig (1993) for the equivalent width of the λ5780.5 Å DIB into estimated values for W_{6284} assuming that the mean ratio measured by Chlewicki et al (1986) and Benvenuti & Porceddu (1989) applies ($W_{6284}/W_{5780} = 2.2$). In Figure 5 we have likewise plotted W_{6284} *vs.* N_{NaI} for both the Galactic data and our starburst data. The starbursts lie at the high-end of the relationship defined by $DIBs$ in the Milky Way.

4.2. Relationship to the λ2175 Å Dust Feature

Over the years, there has been considerable speculation as to a possible connection between the $DIBs$ and the strong and broad feature at λ2175 Å in the Galactic extinction curve (see Benvenuti & Porceddu 1989). In this context, the detection of strong $DIBs$ in starburst spectra is noteworthy. As shown by Calzetti et al (1994), the λ2175 feature is extremely (undetectably) weak in the UV spectra of starbursts. This implies that the carriers of the $DIBs$ and the λ2175 feature must be quite distinct (in agreement with the conclusions of Benvenuti & Porceddu (1989) for the Galactic ISM).

4.3. Speculations

On the face of it, the above results may seem surprising given the extreme differences between the physical conditions in the ISM of intense starbursts and our own Galactic disk.

The strong starbursts in our sample have bolometric surface brightnesses of $\Sigma_{bol} \sim 10^{10}$ to 10^{11} $L_\odot$ kpc^{-2} (e.g. Meurer et al. 1997), typical star-formation rates per unit area of $\Sigma_{SFR} \sim 10$ $M_\odot$ year^{-1} kpc^{-2}, and surface mass densities in gas and stars of $\Sigma_{gas} \sim \Sigma_{stars} \sim 10^9$ $M_\odot$ kpc^{-2} (e.g. Kennicutt 1998). These are roughly 10^3 (Σ_{SFR}), 10^2 (Σ_{gas}) and 10^1 (Σ_{stars}) times larger than the corresponding values in the disks of normal galaxies. These values for Σ_{bol} correspond to a radiant energy density inside the star-forming region that is roughly 10^3 times the value in the ISM of the Milky Way (and see Colbert et al 1999 for direct measurements of this quantity). The rate of mechanical energy deposition (supernova heating) per unit volume in these starbursts is of-order 10^3 times higher than in the ISM of our Galaxy (e.g. Heckman, Armus, & Miley 1990), as is the cosmic ray heating rate (Suchkov, Allen, & Heckman 1993). Finally, simple considerations of hydrostatic equilibrium imply correspondingly high pressures in the ISM: $P \sim G\Sigma_g\Sigma_{tot} \sim$ few $\times$ 10^{-9} dyne cm^{-2} (P/k $\sim$ few $\times$ 10^7 K cm^{-3}, or several thousand times the value in the local ISM in the Milky Way). These high pressures have been confirmed observationally (e.g. Heckman, Armus, & Miley 1990; Colbert et al 1999).

The interesting result of the above is that despite the extreme conditions prevailing inside these starbursts, the dimensionless ratio of the ISM pressure to the energy density in UV photons (or cosmic rays) is quite similar in starbursts and the disk of the Milky Way. This would in turn imply that (for a given ISM temperature) the ratio of the number densities of the gas particles and UV photons (or cosmic rays) would also be similar to their values in the local ISM. Wang, Heckman, & Lehnert (1998) have discussed the evidence that this analysis is correct for the diffuse ionized medium in starbursts and the disks of normal late-type galaxies.

This "homologous" behavior of the ISM in regions spanning over three orders-of-magnitude in heating and cooling rates per particle may help to explain why the ratio of the column density of DIB carriers to that of both Na atoms (Figure 5) and dust grains (Figure 4) appears so similar in extreme starbursts and the ISM of our own Galaxy. In the absence of a well-understood origin for the $DIBs$, further speculation seems premature.

5. Summary

Despite over six decades of investigation, the nature and origin of the Diffuse Interstellar Bands remain a mystery (Herbig 1995). We have presented evidence that - far from being a possibly pathological property of the local ISM in our Galaxy - $DIBs$ are probably ubiquitous in the spectra of far-infrared-bright (dusty) starbursts.

In our own Galaxy, the two most conspicuous $DIBs$ are the features at λ6283.9 Å and λ5780.5 Å. We have detected one or both of these two $DIBs$ in all seven starbursts selected on the basis of strong interstellar $NaI\lambda\lambda$5790,5796 (NaD) absorption from the larger starburst sample studied by Heckman et al (2000 - HLSA). The equivalent widths of these features are $\sim$ 400 to 900 mÅ and $\sim$ 100 to 400 mÅ for the λ6280.9 and λ5780.5 features respectively. These roughly correspond to the greatest DIB strengths observed in the Milky Way (Herbig 1993; Chlewicki et al 1986). In two members of our sample (M82 and NGC2146) the spectra are of high enough signal-to-noise to detect four other weaker $DIBs$ (at 5797.0 Å, 6010.1 Å, 6203.1 Å, and 6613.6 Å). These have typical equivalent widths of $\sim$ 100 mÅ. The relative strengths of these $DIBs$ are rather similar to those in the Milky Way (Herbig 1995; Chlewicki et al 1986; Benvenuti & Porceddu 1989).

The $DIBs$ can be mapped over an extensive region in and around the nuclear starbursts. In the moderately powerful starbursts (L_{bol} = few $\times$ 10^{10} $L_\odot$), this region is $\sim$ 1 kpc in size *vs.* several kpc in the more powerful starbursts (L_{bol} = few $\times$ 10^{11} $L_\odot$). The kinematics of the gas producing the $DIBs$ is evidently more quiescent than that producing the NaD absorption studied by HLSA. In the four starbursts with broad and strongly blueshifted NaD lines, the $DIBs$ are less Doppler-broadened and much less blueshifted (v_{DIB} - v_{sys} $\sim$ -100 km s^{-1}).

In the Milky Way, the $DIBs$ are known to trace a dusty atomic phase of the ISM, since their equivalent widths correlate strongly with the HI column density, the NaI column density, and the reddening parameter $E(B-V)$ (Herbig 1995 and references therein). We show that these starburst $DIBs$ obey the same trends with N_{NaI} and $E(B-V)$ (e.g. W_{6284} $\sim$ 1.2 $E(B-V)$ Å at logN_{NaI} $\sim$ 14 cm^{-2}). Thus, the abundance of the DIB carrier(s) relative to Na atoms and dust grains appears to be very similar in intense starbursts and the diffuse ISM of our own Galaxy.

This seems surprising, given the thousand-fold greater energy density in photons and cosmic rays in the ISM of an intense starburst (e.g. Colbert et al 1999; Suchkov, Allen, & Heckman 1993). However, the gas pressures and densities in the starburst ISM are correspondingly larger as well (e.g. Heckman, Armus, & Miley 1990). Thus, such key dimensionless ratios as gas/photon density and gas-pressure/radiant-energy-density are similar in the ISM of starbursts and the disks of normal spiral galaxies (Wang, Heckman, & Lehnert 1998). This apparent "homology" may help explain the strikingly similar DIB properties.

Finally, we point out that starbursts apparently produce strong $DIBs$ without producing a detectable λ2175 Å dust feature in their UV spectra (Calzetti et al 1994). This underscores the quite distinct origin of the two types of features.

We thank David Neufeld, Ken Sembach, and Don York for useful conversations at various stages of this project. The partial support of this project by NASA grant NAGW-3138 is acknowledged.

REFERENCES

Armus, L., Heckman, T., & Miley, G. 1989, ApJ, 347, 727

Benvenuti, P., & Porceddu, I. 1989, A&A, 223, 329

Bruzual, A.G. & Charlot, S.1993, ApJ, 405, 538

Calzetti, D., Kinney, A., & Storchi-Bergmann, T. 1994, ApJ, 429, 582

Chlewicki, G., van der Zwet, G., van Ijzendoorn, I., & Greenberg, M. 1986, ApJ, 305, 455

Colbert, J, Malkan, M., Clegg, P., Cox, P., Fischer, J., Lord, S., Luhman, M., Satyapal, S., Smith, H., Spinoglio, L., Stacey, G., & Unger, S. 1999, ApJ, 511, 721

di Serego Alighieri, S., & Ponz, J. 1987, in 'ESO Workshop on the SN1987A', ed. I.J. Danziger, ESO Conf. Workshop Proc. No. 26, Garching Bei Munchen: ESO, p. 545

Gallagher, J. & Smith, L. 1999, MNRAS, 304, 540

Hamann, F., Barlow, T., Junkkarinen, V., & Burbidge, E.M. 1997, ApJ, 478, 80

Heckman, T. M., Armus, L., & Miley, G. K. 1990, ApJS, 74, 833

Heckman, T., Lehnert, M., Strickland, D., & Armus, L. 2000 (HLSA), submitted to ApJ

Herbig, G. 1993, ApJ, 407, 142

Herbig, G. 1995, ARA&A, 33, 19

Kennicutt, R. 1998, ApJ, 498, 541

Lehnert, M.., & Heckman, T. 1995, ApJS, 97, 89

Lehnert, M.., & Heckman, T. 1996, ApJ, 472, 546

Leitherer, C., Schaerer, D., Goldader, J., Gonzalez-Delgado, R., Robert, C., Kune, D., De Mello, D., Devost, D., & Heckman, T. 1999, ApJS, 123, 3

Merrill, P. 1934, PASP, 46, 206

Meurer, G., Heckman, T., Leitherer, C., Lowenthal, J., & Lehnert, M. 1997, AJ, 114, 54

Morgan, D. 1987, QJRAS, 28, 328

Salama, F., Galazutdinov, G. A., Krelstrokowski, J., Allamandola, L. J., & Musaev, F. A. 1999, ApJ, 526, 265

Sonnentrucker, P., Cami, J., Ehrenfreund, P., & Foing, B. H. 1997, A&A, 327, 1215

Spitzer, L. 1968, "Diffuse Matter in Space", (Interscience: New York)

Suchkov, A., Allen, R., & Heckman, T. 1993, ApJ, 413, 542

Wang, J., Heckman, T., & Lehnert, M. 1998, ApJ, 509, 93

This preprint was prepared with the AAS LaTeX macros v4.0.

Table 1. Basic Properties

Galaxy (1)	W_{6284} (2)	W_{5780} (3)	Ang. Size (4)	Size (5)	$E(B-V)$ (6)	$\log N_{NaI}$ (7)
NGC1614	940±40	100:	11	3.5	0.9	14.1
NGC1808	550±40	140:	17	1.2	0.9	14.3
NGC2146	940±30	360	28	1.8	0.9	13.8
M82	880±30	240	55	0.9	1.0	13.9
NGC3256	370±40	100:	18	3.0	0.6	13.8
IRAS10565+2448	530±90	...	5	4.5	0.7	14.0
NGC6240	...	640±70	12	6.0	1.2	13.9

Note. Col. (2) The equivalent width of the λ6283.9 DIB in mÅ. Col. (3) The equivalent width of the λ5780.5 DIB in mÅ. The uncertainty is due primarily to the accuracy with which contamination by the stellar photospheric CrI+CuIλ5782 can be removed. We estimate this leads to an uncertainty of $\pm$50mÅ. The detection of this DIB is therefore only tentative in NGC1614, NGC1808, and NGC3256 (indicated by a colon). Col. (4) The angular size (in arcsec) over which the λ6283.9 DIB is detectable (the λ5780.5 DIB was used in NGC6240). Col. (5) The corresponding physical size (in kpc), for our adopted $H_0 = 70$ km s^{-1} Mpc^{-1}. Col. (6) The estimated color excess along the line-of-sight to the stellar continuum, based on the observed continuum color and a model starburst spectral energy distribution (Leitherer et al 1999; see HLSA for details). Col. (7) The logarithm of the estimated column density of NaI atoms (cm^{-2}). These were derived using the standard doublet ratio technique (Spitzer 1968) and its variant in Hammann et al (1997). See HLSA for details. Based on an intercomparison of the values obtained by different techniques, we estimate the uncertainty to be $\pm$0.2 dex.

Table 2. Weaker DIBs

Galaxy (1)	W_{5780} (2)	W_{5797} (3)	W_{6010} (4)	W_{6203} (5)	W_{6283} (6)	W_{6613} (7)	Δ (8)
NGC2146	360	100	130	160	910	120	30
M82	240	70	110	120	880	120	30

Note. — See Figure 2. All equivalent widths are given in mÅ. Col. (8) Uncertainties in mÅ.

Table 3. Kinematic Properties

Galaxy (1)	Δv_{DIB} (2)	Δv_{NaD} (3)	v_{sys} (4)	v_{DIB} (5)	v_{NaD} (6)
NGC1614	300(7.7±0.6)	420	4760	4657	4636
NGC1808	240(6.7±0.6)	300	1001	1040	1013
NGC2146	160(5.3±0.4)	140	916	932	930
M82	160(5.3±0.4)	170	214	268	204
NGC3256	220(6.4±0.6)	550	2801	2755	2489
IRAS10565+2448	370(9.3±1.0)	500	12923	12840	12717
NGC6240	430(8.9±1.0)	600	7339	7232	7049

Note. Col. (2) The Doppler broadening (full-width-at-half maximum) in km s^{-1} for the λ6283.9 DIB (the λ5780.5 DIB was used in NGC6240). These widths have been corrected for the intrinsic width of the DIB feature (see text) and for the instrumental resolution of the spectrograph (see HLSA). The raw, measured line widths and their associated uncertainties (in Å) are given in parantheses. Col. (3) The full-width-at-half-maximum in km s^{-1} of the members of the $NaI\lambda\lambda$5890,5896 doublet (NaD). Uncertainties are $\pm$20 km s^{-1}. Taken from HLSA. Col. (4) The heliocentric galaxy systemic velocity. Approximate uncertainties range from $\pm$10 km s^{-1} for NGC1808, NGC2146, and M82 to $\pm$50 km s^{-1} for NGC1614 and NGC3256, to $\pm$100 km s^{-1} for NGC6240 and IRAS10565+2448. See HLSA and references therein. Col. (5) The heliocentric velocity of the λ6283.9 DIB (the λ5780.5 DIB was used in NGC6240). The measurement uncertainties are $\pm$30 km s^{-1} for NGC2146 and M82, $\pm$50 km s^{-1} for NGC1614, NGC1808, and NGC3256, and $\pm$80 km s^{-1} for IRAS10565+2448 and NGC6240. These do not include any uncertainties in the true value of the rest wavelength for the DIB. Col. (6) The heliocentric velocity of the NaD doublet taken from HLSA. Uncertainties are $\pm$20 km s^{-1}.

Fig. 1.— The spectrum of the nucleus of M82 before (top) and after (bottom) the subtraction of the scaled spectrum of K giant star. This subtraction removes the stellar photospheric absorption features whose presence complicates the detection and measurement of the $DIBs$ in our sample of starbursts. See text for details.

Fig. 2.— Spectra of the DIB at $\lambda_{rest} = 6283.9$ Å in six starburst nuclei and of the DIB at $\lambda_{rest} = 5780.5$ Å in NGC6240 (denoted by tick marks). These spectra have been normalised to unit intensity, cleaned of photospheric absorption-lines due to cool stars by subtraction of a suitably-normalized spectrum of a K giant star, and then diluted by the addition of featureless continuum equal in strength to the subtracted starlight. See Figure 1 for an example of the effect of K-star subtraction on the spectrum of M82. The absorption feature at $\lambda_{observed} \sim 6278$ Å in NGC1808, NGC2146, and M82 is telluric O_2. See text for details.

Fig. 3.— Spectra of the nuclei of NGC2146 and M82 showing other $DIBs$. The spectra have been processed as described in Figure 2 (see text). The detected features are indicated by five tick marks denoting the $DIBs$ at $\lambda_{rest} = 5780.5$ Å 5797.0 Å, 6010.1 Å, 6203.1 Å, and 6283.9 Å. The unmarked absorption feature at $\lambda_{observed} \sim 6278$ Å is telluric O_2. See Table 2.

Fig. 4.— The equivalent width of the Diffuse Interstellar Band at λ_{rest} =6283.9 Å (in mÅ) is plotted *vs.* the color excess $E(B-V)$ for a large sample of Galactic stars (hollow points) and our starburst nuclei (larger solid points). The Galactic data come from Benvenuti & Porceddu (1989), Chlewicki et al (1986), and Herbig (1993). Since Herbig gave only the equivalent widths for the weaker DIB at λ5780.5 Å we have converted these values to W_{6284} assuming the mean ratio measured by Benvenuti & Porceddu (1989) and Chlewicki et al (1986): $< W_{6284}/W_{5780} > = 2.2$. We have done likewise for NGC6240 in which the λ 6283.9 feature is buried under a strong and broad [OI]λ6300 nebular emission-line (see Figure 3). Note that the starburst nuclei lie along the relationship defined by the Galactic sight-lines.

Fig. 5.— The logarithm of the equivalent width of the Diffuse Interstellar Band at λ_{rest} =6283.9 Å (in mÅ) is plotted *vs.* the logarithm of the NaI column density or a large sample of Galactic stars (hollow points) and our starburst nuclei (larger solid points). The Galactic data come from Herbig (1993). Since Herbig gave only the equivalent widths for the weaker DIB at λ5780.5 Å we have converted these values to W_{6284} assuming the mean ratio measured by Benvenuti & Porceddu (1989) and Chlewicki et al (1986): $< W_{6284}/W_{5780} > = 2.2$. We have done likewise for NGC6240 in which the λ 6283.9 feature is buried under a strong and broad [OI]λ6300 nebular emission-line (see Figure 3). Note that the starburst nuclei lie at the upper end of the relationship defined by the Galactic sight-lines.

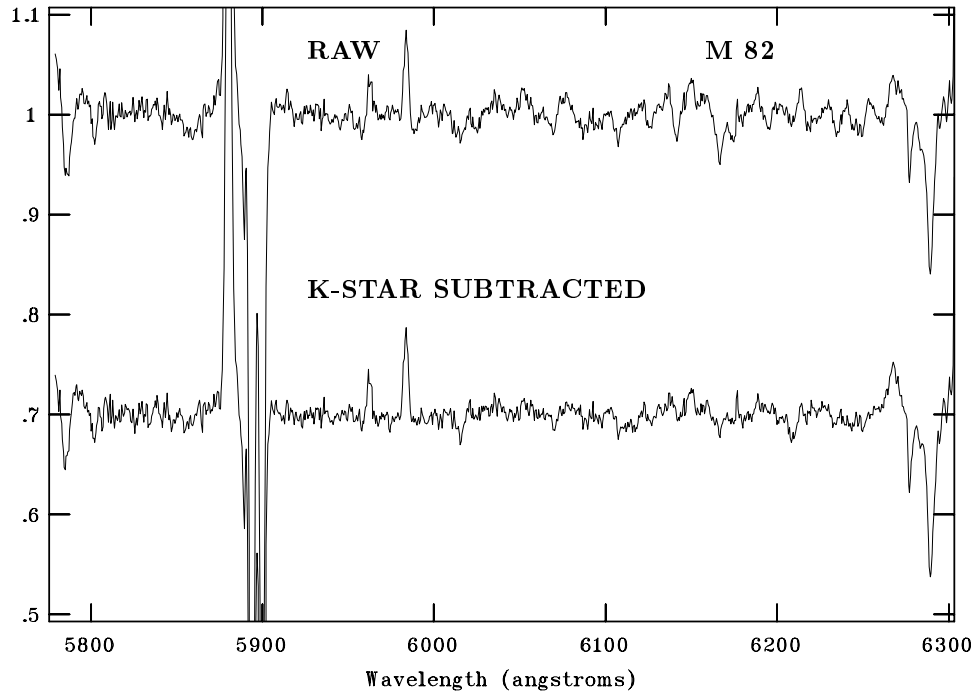
RAW
M 82
K-STAR SUBTRACTED
1.1
1
.9
.8
.7
.6
.5
5800
5900
6000
6100
6200
6300
Wavelength (angstroms)

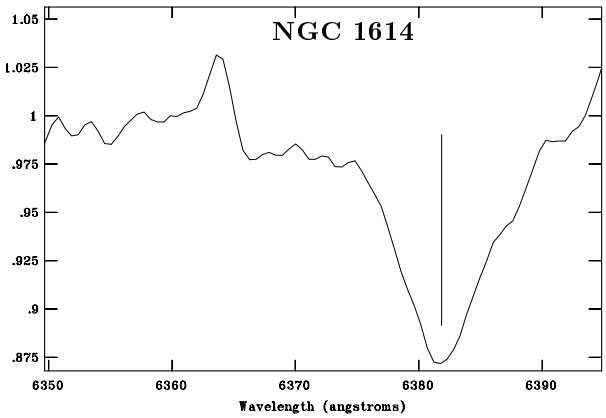
NGC 1614
1.05
1.025
1
.975
.95
.925
.9
.875
6350
6360
6370
6380
6390
Wavelength (angstroms)

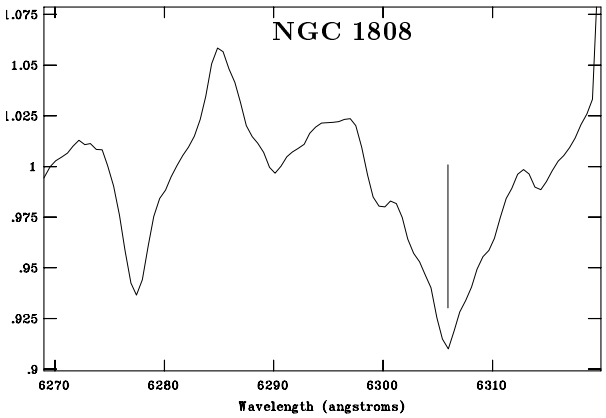
NGC 1808
1.075
1.05
1.025
1
.975
.95
.925
.9
6270
6280
6290
6300
6310
Wavelength (angstroms)

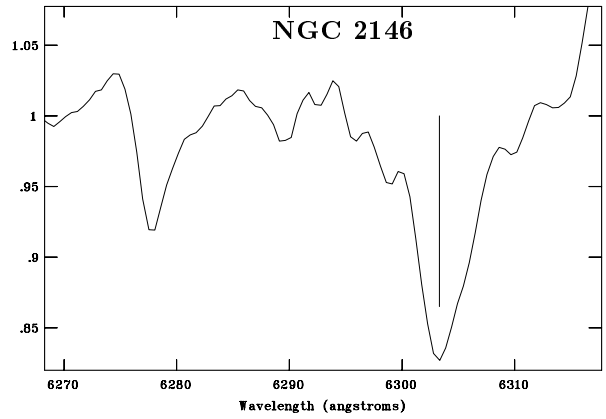
NGC 2146
1.05
1
.95
.9
.85
6270
6280
6290
6300
6310
Wavelength (angstroms)

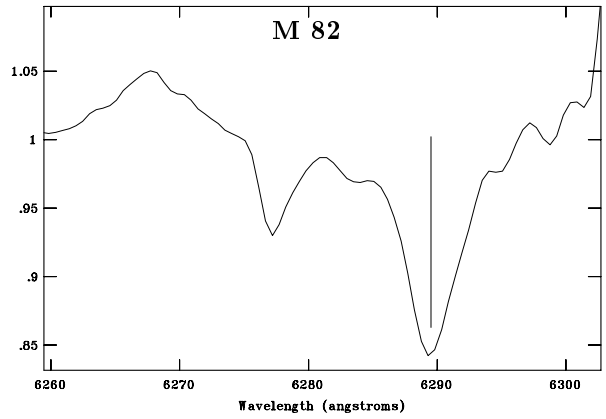
M 82
1.05
1
.95
.9
.85
6260
6270
6280
6290
6300
Wavelength (angstroms)

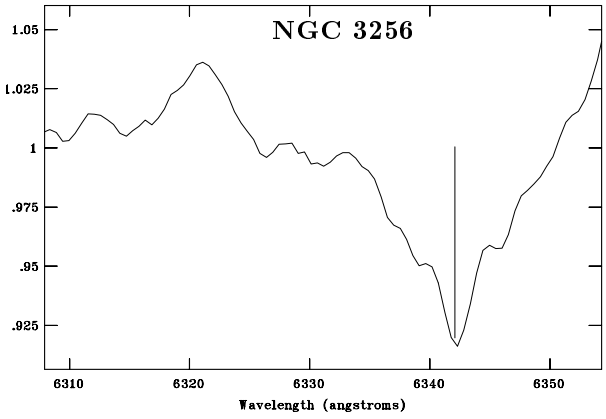
NGC 3256
1.05
1.025
1
.975
.95
.925
6310
6320
6330
6340
6350
Wavelength (angstroms)

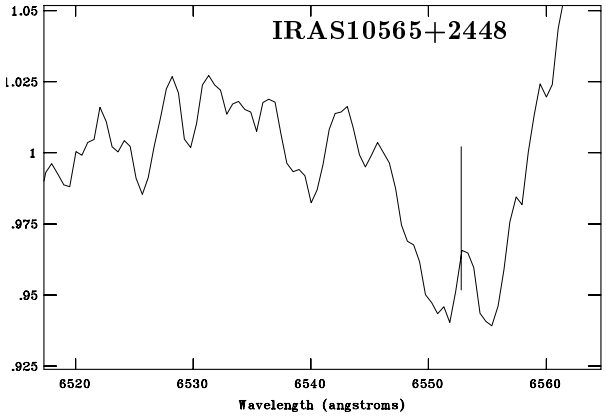
IRAS10565+2448
1.05
1.025
1
.975
.95
.925
6520
6530
6540
6550
6560
Wavelength (angstroms)

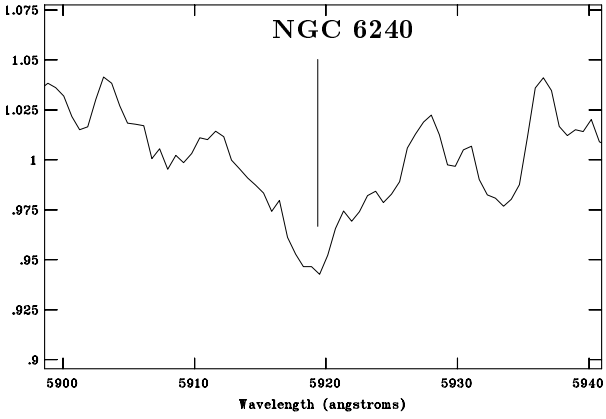
NGC 6240
1.075
1.05
1.025
1
.975
.95
.925
.9
5900
5910
5920
5930
5940
Wavelength (angstroms)

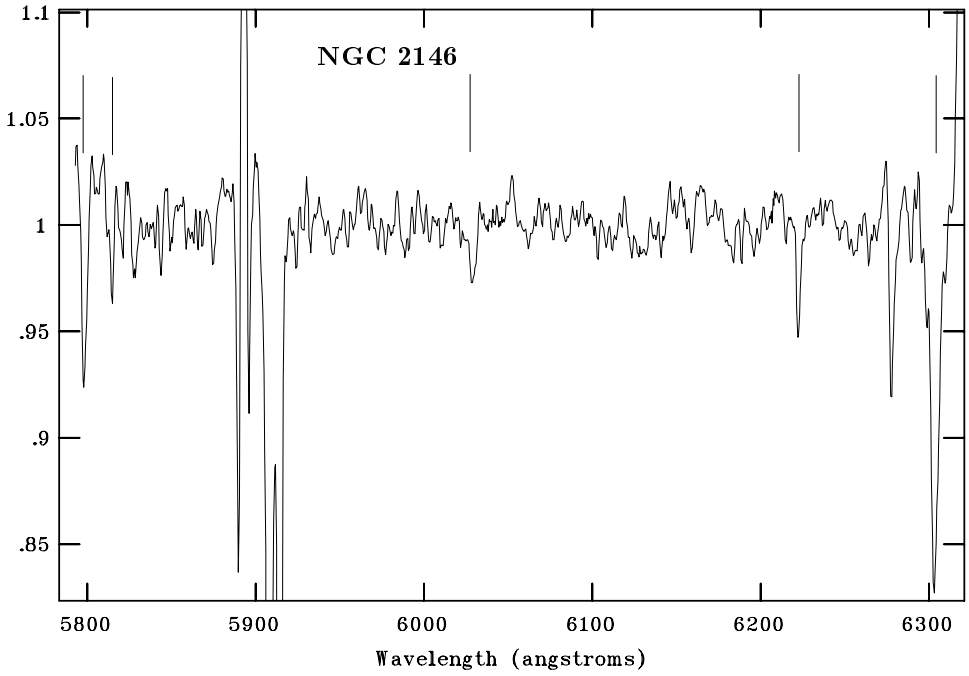
NGC 2146
1.1
1.05
1
.95
.9
.85
5800
5900
6000
6100
6200
6300
Wavelength (angstroms)

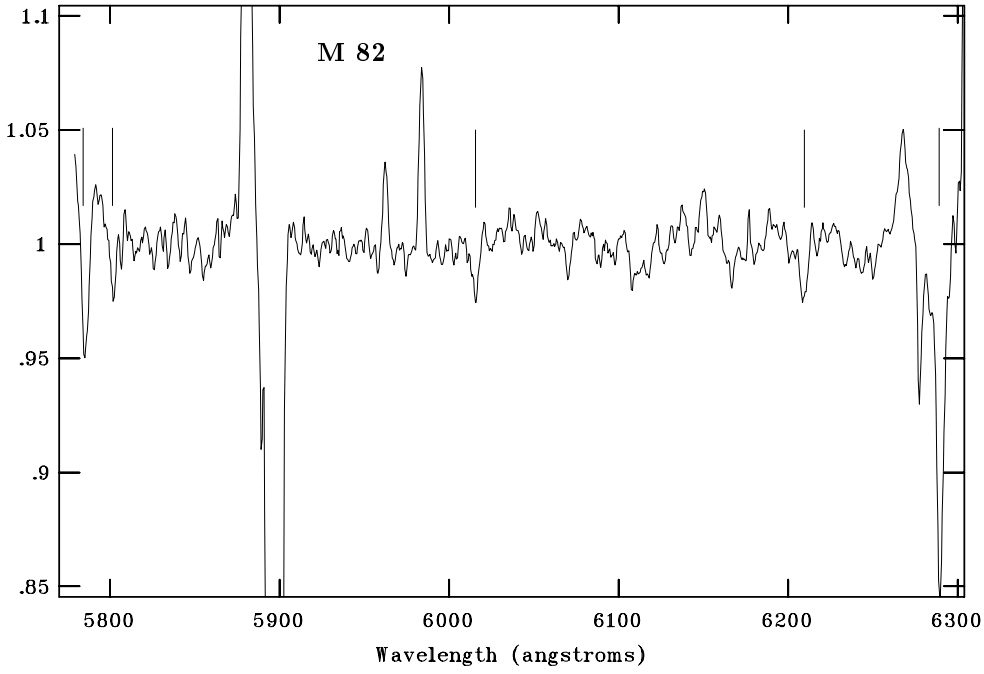
M 82
1.1
1.05
1
.95
.9
.85
5800
5900
6000
6100
6200
6300
Wavelength (angstroms)

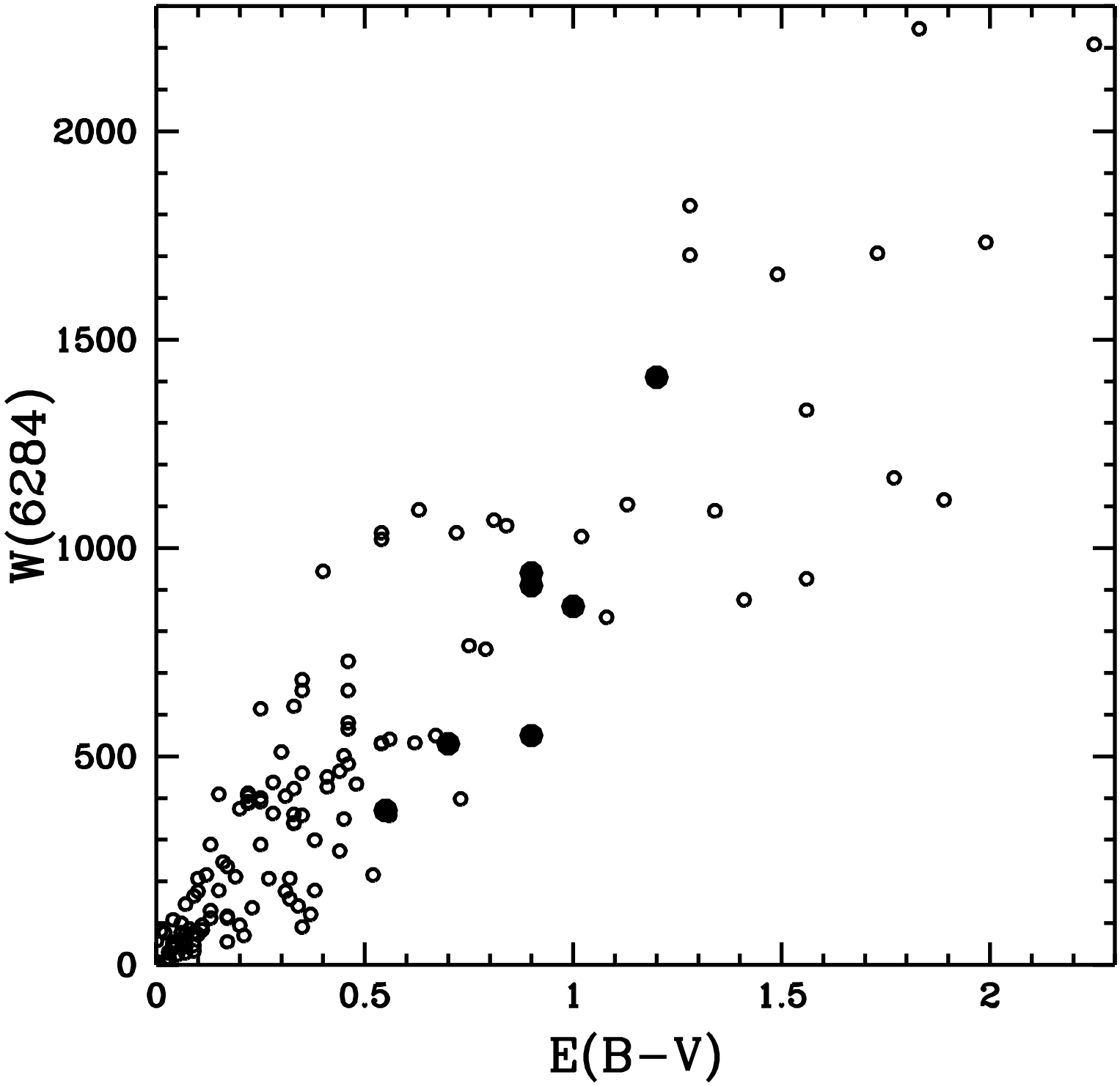
2000
1500
1000
500
0
W(6284)
0
0.5
1
1.5
2
E(B−V)

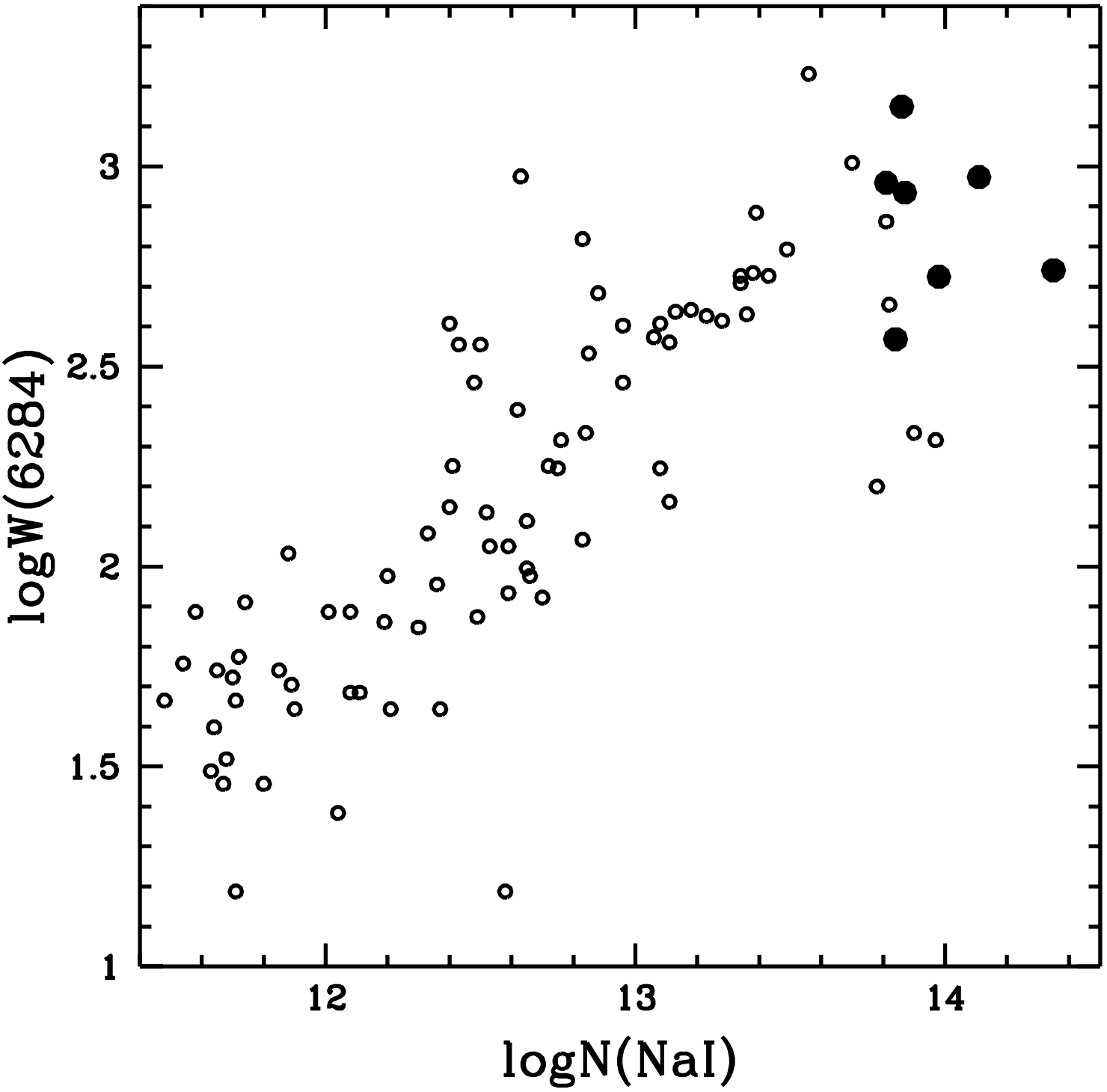
logW(6284)
logN(NaI)
1
1.5
2
2.5
3
12
13
14